

Bioconjugation of Papain on Superparamagnetic Nanoparticles Decorated with Carboxymethylated Chitosan

Yuan-Yuan Liang and Li-Ming Zhang*

Laboratory for Polymer Composite and Functional Materials, Institute of Optoelectronic and Functional Composite Materials, School of Chemistry and Chemical Engineering, Sun Yat-Sen (Zhongshan) University, Guangzhou 510275, China

Received November 16, 2006; Revised Manuscript Received February 15, 2007

Functionalized Fe_3O_4 nanoparticles decorated with carboxymethylated chitosan were developed and used as a novel magnetic support for the covalent conjugation of papain, one of the most important industrial proteases. The analyses of transmission electron micrographs (TEM) and X-ray diffraction (XRD) showed that the size and structure of functionalized Fe_3O_4 nanoparticles had no significant changes after conjugation with papain. Magnetic measurement revealed that the resultant papain-conjugated nanoparticles were superparamagnetic with a saturation magnetization of 59.3 emu/g. Analyses of Fourier transform infrared (FTIR) spectroscopy and measurement of ζ potentials confirmed the conjugation of papain with the functionalized Fe_3O_4 nanoparticles. Compared with the native papain, the conjugated papain was found to exhibit enhanced enzyme activity, better tolerance to the variations of medium pH and temperature, and improved storage stability as well as good reusability. Considering that the magnetic separation technique possesses the advantages of rapidity, high efficiency, cost-effectiveness, and lack of negative effect on biological activity, such a bioconjugate system may hold potential applications in food, pharmaceutical, leather, cosmetic, and textile industries.

Introduction

As one of the most important industrial proteases, papain, consisting of a single peptide chain of 211 amino acid residues folded into two parts that form a cleft and having 11 lysine residues, has been widely used in food, pharmaceutical, leather, cosmetic, and textile industries.^{1–3} To enhance the enzymatic activity, lifetime, and stability of papain, various supports such as mesoporous silica,⁴ mesoporous molecular sieve,⁵ cold-plasma functionalized polyethylene and glass surfaces,⁶ macroporous bead carrier of copolymer,⁷ modified poly(ether)sulfone membranes,⁸ epoxy polymer,⁹ porous poly(methyl L-glutamate) beads,¹⁰ polyacrolein microspheres,¹¹ and anion-exchange resins¹² have been investigated and used for the immobilization of papain.

In recent years, nanoscale materials have been found to have great potential to serve as superior enzyme supports due to their large surface-to-volume ratios in comparison with traditional macroscale materials.^{13–15} In particular, use of magnetic nanoparticles as a support for immobilized enzymes has achieved growing attraction because of the following advantages: (i) higher specific surface area obtained for the binding of a larger amount of enzymes, (ii) lower mass transfer resistance and less fouling, and (iii) selective separation of immobilized enzymes from a reaction mixture by application of a magnetic field.¹⁶ For example, Huang et al.¹⁷ carried out direct binding and characterization of lipase onto magnetic nanoparticles without surface modification; Dyal et al.¹⁸ reported the stability and enzymatic activity of *Candida rugosa* lipase immobilized on Fe_2O_3 magnetic nanoparticles. Up to now, however, no study has dealt with the immobilization of papain on magnetic nanoparticle supports.

In this work, we explored a new kind of nanoscale magnetic support, functionalized superparamagnetic Fe_3O_4 nanoparticles decorated with carboxymethylated chitosan, to immobilize and stabilize papain. For this purpose, the size, structure, and magnetic properties of the magnetic nanoparticles without and with conjugated papain were examined. In particular, the activity, stability, and kinetic behavior of the conjugated enzyme were investigated.

Experimental Section

Materials. Papain (EC 3.4.22.2) from *Carica papaya* and casein were purchased from Shanghai Bo Ao Biochemical Co. Ltd. (China). Chitosan with deacetylation degree of 85.0% and viscosity-average molecular weight of 350K, *N*-hydroxysuccinimide (NHS), and 1-ethyl-3-(3-dimethylaminopropyl)carbodiimide [$\text{H}_5\text{C}_2-\text{N}=\text{C}=\text{N}-(\text{CH}_2)_3-\text{N}(\text{CH}_3)_2$, EDC] were purchased from Aldrich. Succinic anhydride, iron(II) chloride tetrahydrate (99%), and iron(III) chloride hexahydrate (98%) were purchased from Guangzhou Chemical Co. (China). All the chemicals were used as received without further treatment. The water used in this work was Milli-Q ultrapure water.

Preparation of Magnetic Nanoparticles and Their Surface Modification. Fe_3O_4 magnetic nanoparticles were prepared by coprecipitating iron(II) and iron(III) in alkaline solution and then treating under hydrothermal conditions. At first, 0.30% aqueous iron(II) chloride tetrahydrate dispersion and 0.85% iron(III) chloride hexahydrate dispersion were thoroughly mixed and added to 8.0 mol/L NaOH under continuous stirring at room temperature. Then, the reaction mixture was heated at 80 °C for 30 min, and the medium pH was maintained at 10 by the addition of aqueous NaOH during the reaction. In order to remove the chloride ions, aqueous solution of silver nitrate was added until no white precipitate occurred. After that, the resulting magnetic nanoparticles was washed with distilled water and ethanol and dried in a vacuum oven at 70 °C.

The surface modification of resulting Fe_3O_4 nanoparticles was carried out by the carboxymethylation of chitosan and subsequent covalent

* To whom correspondence should be addressed: e-mail ceszhlm@mail.sysu.edu.cn.

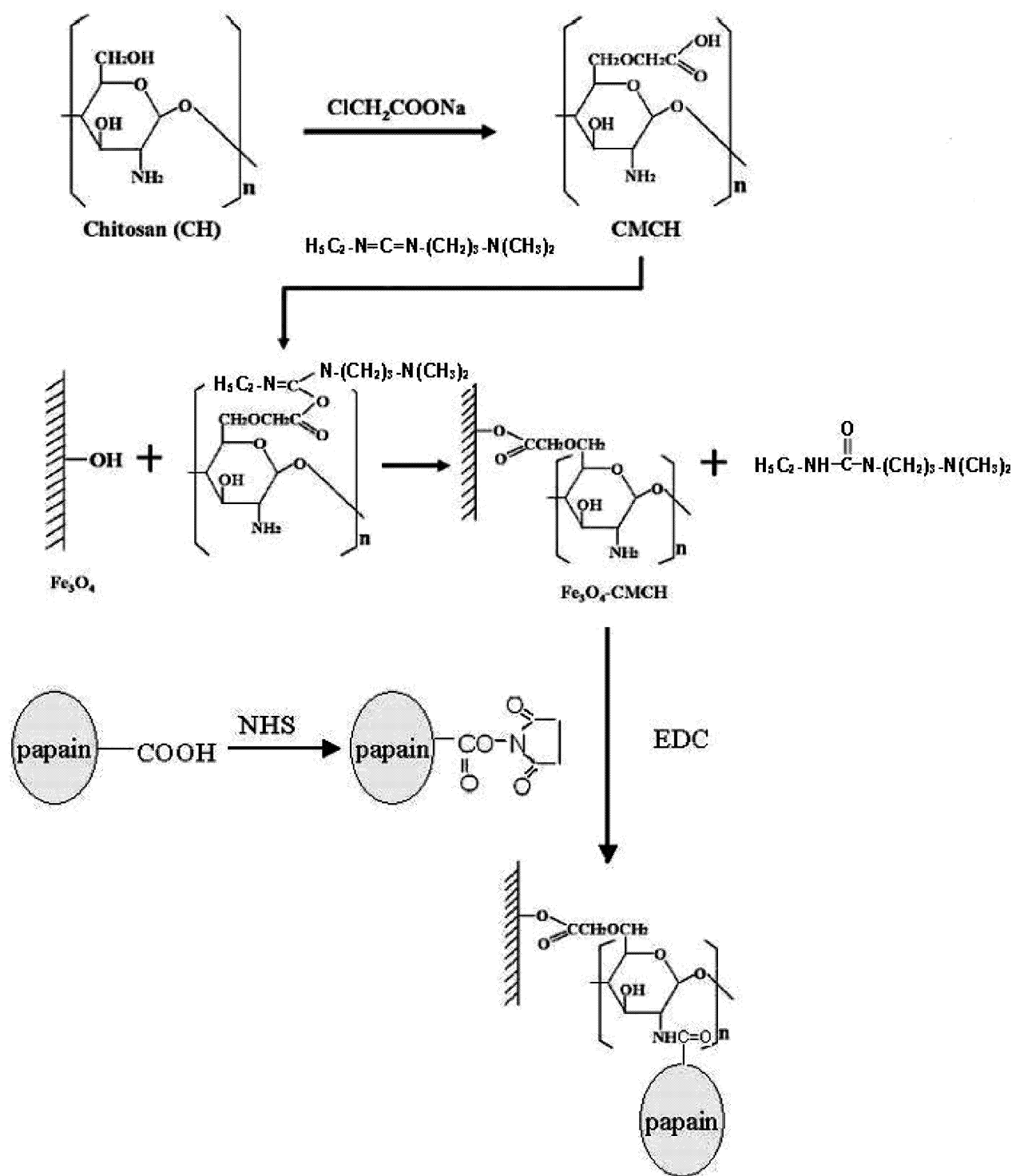


Figure 1. Schematic illustration for the surface modification of Fe_3O_4 magnetic nanoparticles by carboxymethylated chitosan (CMCH) and subsequent conjugation with papain.

binding onto Fe_3O_4 nanoparticles via EDC. For the carboxymethylation of chitosan,¹⁹ 3.0 g of chitosan and 15.0 g of sodium hydroxide were added into 100 mL of 2-propanol/water (80/20 v/v) mixture at 60 °C to swell and alkalinize for 1.0 h. Then, 20 mL of monochloroacetic acid solution (0.75 g/mL in 2-propanol) was added into the reaction mixture dropwise over 30 min. After reaction for 4.0 h at 60 °C, 200 mL of ethyl alcohol was added to stop the reaction. Finally, the solid was filtered, washed with ethyl alcohol to remove salt and water, and dried in a vacuum oven at 55 °C. For the covalent conjugation,²⁰ 75 mg of the magnetic nanoparticles was added to 4 mL of phosphate buffer (0.2 mol/L $\text{Na}_2\text{HPO}_4\text{--NaH}_2\text{PO}_4$, pH 6.0) containing 25 mg of EDC, and then the reaction mixture was ultrasonicated for 10 min. After that,

1.0 mL of carboxymethylated chitosan solution (25 mg/mL in phosphate buffer) was added, and the reaction mixture was ultrasonicated for another 1.0 h. The product was recovered from the reaction mixture by a permanent magnet (6000 G) and then washed with water and ethanol.

Conjugation of Papain. To immobilize papain on the carboxymethylated chitosan-modified Fe_3O_4 ($\text{Fe}_3\text{O}_4\text{--CMCH}$) nanoparticles, papain (2.5–6 mg), EDC (5 mg), and NHS (6 mg) were dissolved in 5 mL of phosphate buffer (pH 6.0, 2 mmol/L). After that, 10 mg of $\text{Fe}_3\text{O}_4\text{--CMCH}$ was added. The mixed suspension was then sonicated at 4 °C for 10 min and shaken at room temperature for 24 h. The papain-conjugated $\text{Fe}_3\text{O}_4\text{--CMCH}$ was recovered from the reaction mixture

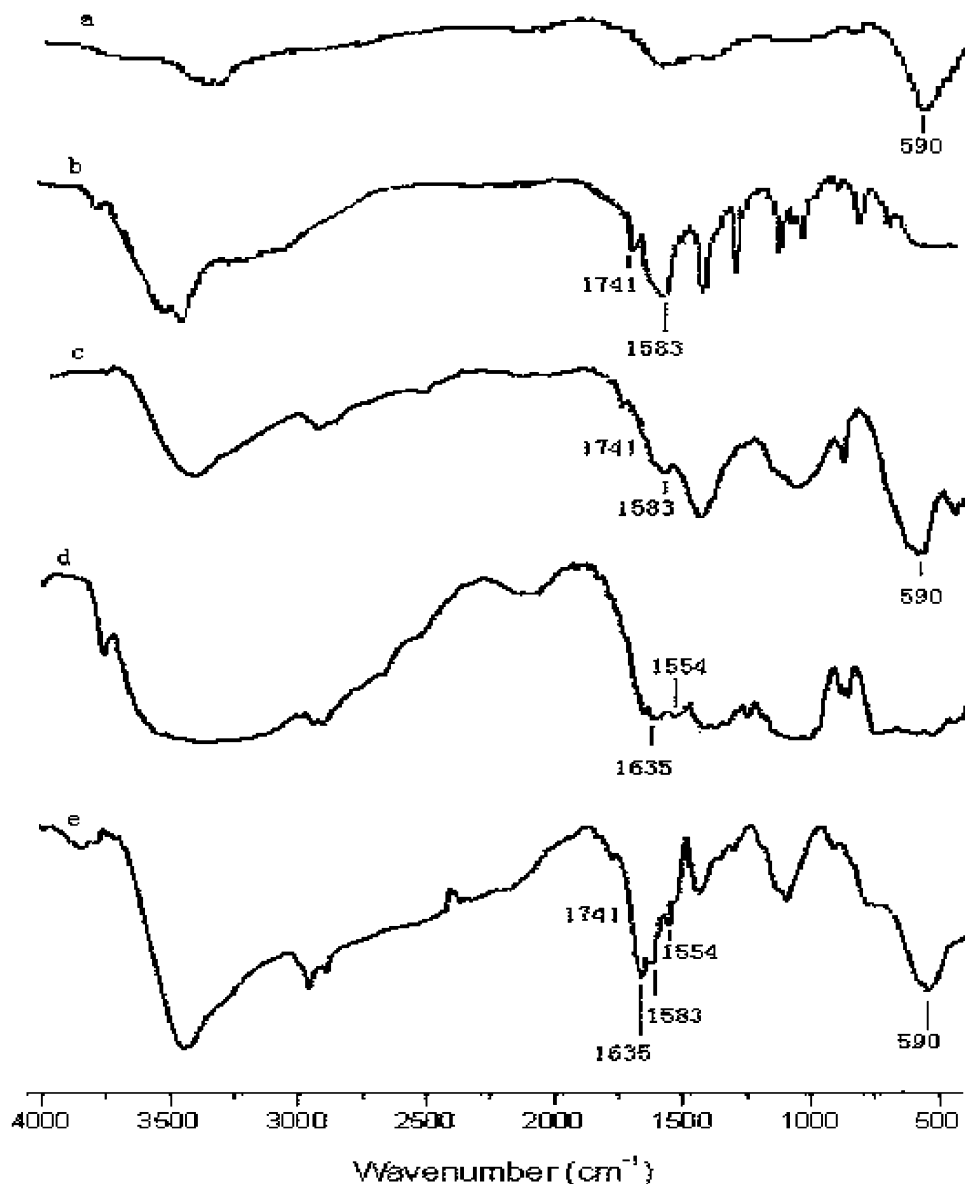


Figure 2. FTIR spectra for naked Fe_3O_4 nanoparticles (a), CMCH (b), unconjugated Fe_3O_4 -CMCH nanoparticles (c), native papain (d), and conjugated Fe_3O_4 -CMCH nanoparticles (e).

by placing the bottle on a permanent magnet with a surface magnetization of 6000 G. The supernatant was used to determine the content of unconjugated papain. The precipitates were washed with 2 mmol/L phosphate buffer (pH 6.0) and used for the measurement of activity and stability.

Characterization. Conjugation of papain on Fe_3O_4 -CMCH nanoparticles was confirmed by Fourier transform infrared (FTIR) analyses on a Nexus 670 model FTIR spectrophotometer. The morphology and size of the Fe_3O_4 -CMCH nanoparticles without and with conjugated papain were observed by a JEM-100CX II transmission electron microscope (Japan). X-ray diffraction (XRD) measurements were performed on a D/MAX 2200 VPC X-ray diffractometer (Japan) using $\text{Cu K}\alpha$ radiation. The magnetic measurements were done with a superconducting quantum interference device (SQUID) model MPMS XI-7 magnetometer (USA) with a maximum magnetic field of 7 T and a sensibility of 10^{-6} emu. The ζ potentials for aqueous dispersions of the Fe_3O_4 -CMCH nanoparticles before and after conjugation with papain were measured by use of a Powereach JS94H microelectrophoresis unit (China).

Activity Measurements. The activity of the conjugated papain was determined by using casein as the substrate.^{2,21,22} For this purpose, activation of the papain was first carried out according to the following

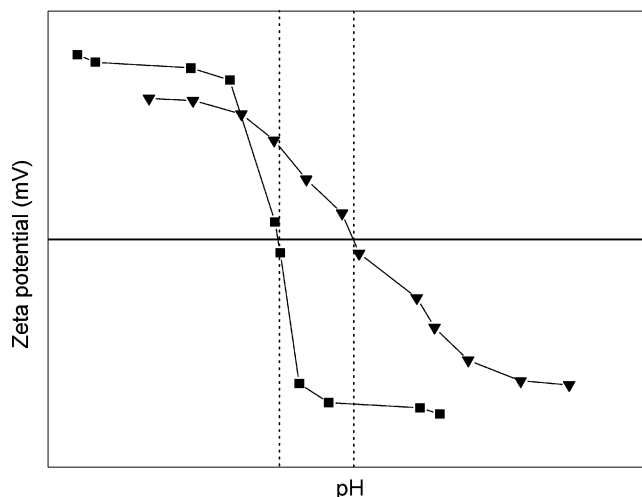


Figure 3. ζ potentials for aqueous dispersions of Fe_3O_4 -CMCH nanoparticles before (■) and after (▼) conjugation with papain.

procedure: The conjugated papain in 50 mmol/L phosphate buffer was mixed with 50 mmol/L L-cysteine hydrochloride and 3 mmol/L

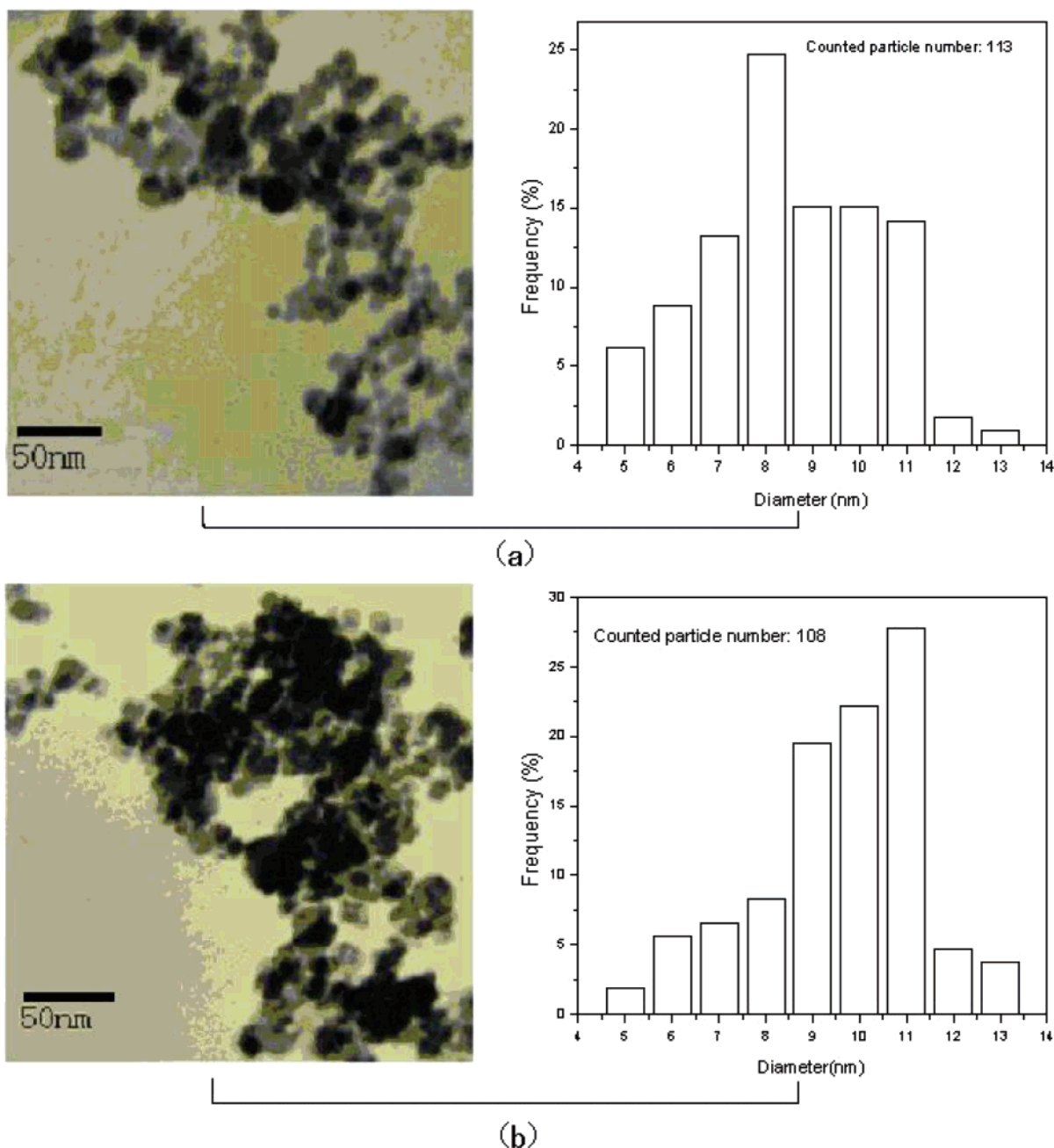


Figure 4. TEM micrographs and size distributions of Fe_3O_4 -CMCH nanoparticles before (a) and after (b) conjugation with papain.

ethylenediaminetetraacetic acid (EDTA) and incubated for 30 min at 30 °C. After the centrifugation, the supernatant was taken for further experiments. An aliquot (0.5 mL) of such activated papain was added to the test tube containing 0.5 mL of casein (2%) solution. The reaction was carried out at a certain temperature for 10 min and stopped by the addition of 1 mL of 15% trichloroacetic acid (TCA). The liquid solution was separated from the conjugated papain via a permanent magnet (6000 G), and 5 mL of 0.5 mol/L Na_2CO_3 was added to 0.5 mL of such solution and kept for 10 min. After that, 0.5 mL of Folin Ciocalteu's reagent was added. The tubes were incubated for 30 min in the dark for color development. The color was read against the reagent blank at 660 nm in a 721 spectrophotometer (China). The activity was expressed as the amount of enzyme required to release 1 μg of tyrosine per minute per milliliter. In the case of native papain, the activity measurement was done following the procedures and conditions similar to those for conjugated papain, except that native papain was used and magnetic separation was unnecessary.

Results and Discussion

Figure 1 gives a schematic illustration for the surface modification of Fe_3O_4 magnetic nanoparticles by carboxymethylated chitosan (CMCH) and subsequent conjugation with papain. The biocompatible CMCH coating not only rendered the magnetic nanoparticles water-soluble but also allowed the magnetic nanoparticles to be bioconjugated with papain molecules by its functional moieties. Figure 2 shows FTIR spectra for naked Fe_3O_4 nanoparticles, CMCH, and Fe_3O_4 -CMCH nanoparticles before and after conjugation with papain as well as for native papain. As seen, the spectrum of Fe_3O_4 -CMCH nanoparticles before conjugation (Figure 2c) shows not only the main characteristic band of the naked pure Fe_3O_4 nanoparticles at 590 cm^{-1} (Figure 2a) but also the characteristic peaks of CMCH at 1741 cm^{-1} (corresponding to the carboxyl groups) and 1583 cm^{-1} (corresponding to the amino groups)

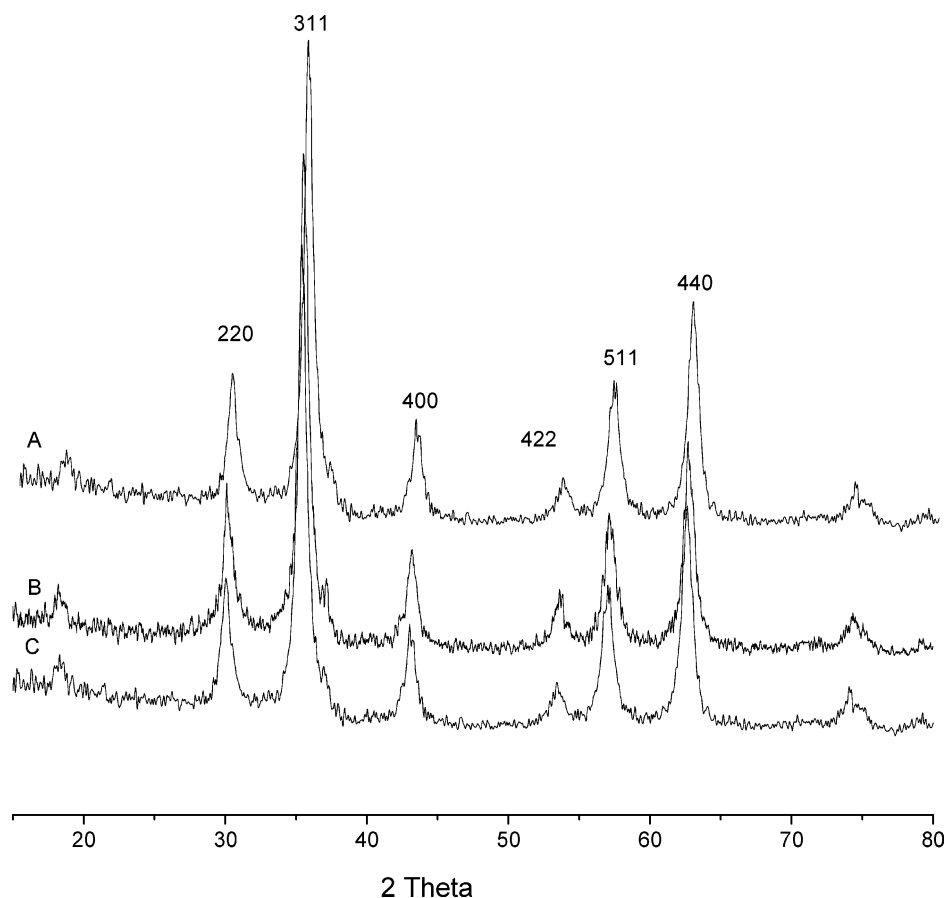


Figure 5. XRD patterns for pure Fe_3O_4 nanoparticles (A) and for Fe_3O_4 -CMCH nanoparticles before (B) and after (C) conjugation with papain.

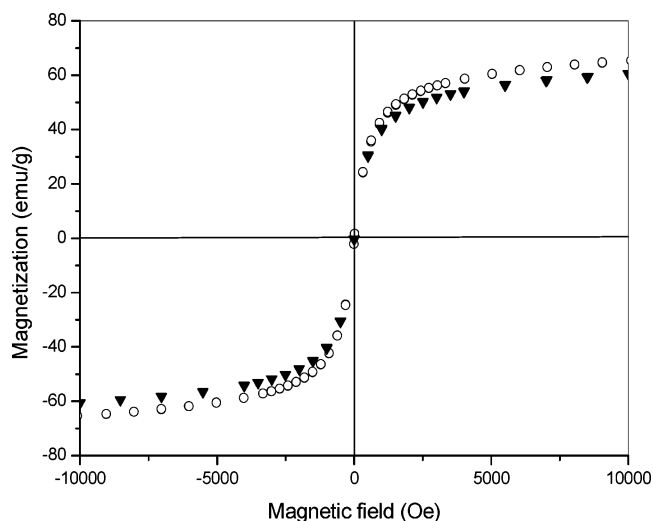


Figure 6. Plots of magnetization versus magnetic field at 300 K for Fe_3O_4 -CMCH nanoparticles without (○) and with (▼) conjugated papain at 300 K.

(Figure 2b). After conjugation with papain, the spectrum of the resultant nanoparticles (Figure 2e) shows not only the characteristic bands of the original Fe_3O_4 -CMCH nanoparticles at 590, 1741, and 1583 cm^{-1} (Figure 2c) but also the characteristic peaks of the native papain at 1635 cm^{-1} (—CONH amide band II) and 1554 cm^{-1} (—NH amide band II)²³ (Figure 2d). Furthermore, the absorption of amide band II at 1635 cm^{-1} increased, which may be due to the formation of the amide linkage between the amino group on the Fe_3O_4 -CMCH nanoparticles and the carboxyl group of papain after being activated by *N*-hydroxysuccinimide (NHS). In addition, we

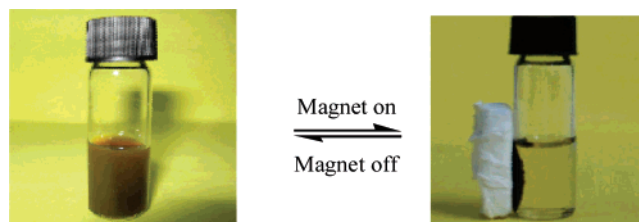


Figure 7. Magnetic-field-assisted separation for papain conjugated with Fe_3O_4 -CMCH nanoparticles in phosphate buffer.

measured the ζ potentials for aqueous dispersions of Fe_3O_4 -CMCH nanoparticles before and after conjugation with papain, and we found that the isoelectric point of unconjugated Fe_3O_4 -CMCH nanoparticles was about 5.45, while the isoelectric point of conjugated Fe_3O_4 -CMCH nanoparticles was shifted to 6.16, as shown in Figure 3. These facts confirm the conjugation of papain with the Fe_3O_4 -CMCH nanoparticles.

Typical TEM micrographs and size distributions for Fe_3O_4 -CMCH nanoparticles before and after conjugation with papain are shown in Figure 4. The particle sizes were determined by measuring the lengths over 100 particles within different regions of a given TEM grid containing the dispersion. In the case of unconjugated nanoparticles, the histogram of such a measured region includes 113 particle measurements. In the case of conjugated nanoparticles, the histogram of such a measured region includes 108 particle measurements. Fe_3O_4 -CMCH nanoparticles without conjugated papain were essentially spherical and monodisperse, with a mean diameter of 8.5 nm. After conjugation with papain, the nanoparticles remained spherical and monodisperse and had a mean diameter of 9.6 nm. This reveals that the conjugation process did not significantly result in agglomeration and change in size of the nanoparticles, which

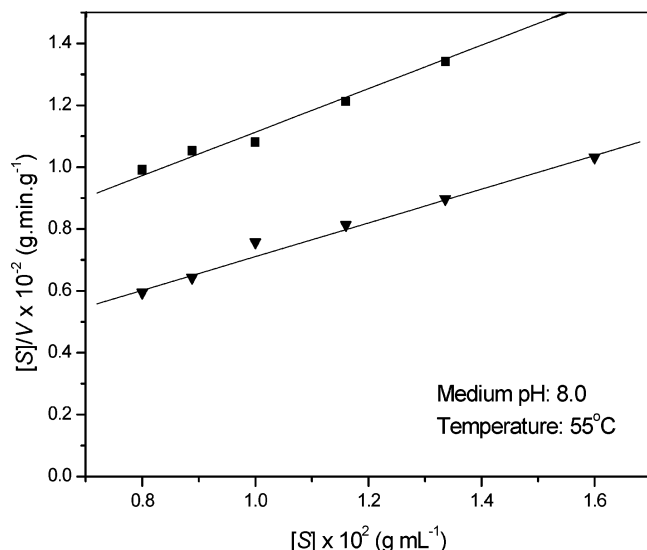


Figure 8. Hanes–Woolf plots for the hydrolysis of casein as the substrate in the presence of native papain (■) and papain conjugated with Fe_3O_4 –CMCH nanoparticles (▼).

Table 1. Activity Retention of Native and Conjugated Papain at Different pH Values (55 °C)

pH value	native papain (%)	conjugated papain (%)
6.0	62.3	73.7
7.0	98.0	80.3
8.0	86.7	99.2
9.0	82.3	89.8
10.0	73.2	85.5
11.0	69.2	79.6

Table 2. Activity Retention of Native and Conjugated Papain at Different Temperatures (pH 8.0)

temp (°C)	native papain (%)	conjugated papain (%)
45	85.7	85.3
55	99.2	96.4
65	96.1	97.3
75	82.6	99.5
85	73.2	89.4

could be attributed to the fact that the reaction occurred only on the Fe_3O_4 –CMCH nanoparticle surface. Figure 5 shows the XRD patterns for pure Fe_3O_4 , Fe_3O_4 –CMCH nanoparticles, and papain-conjugated Fe_3O_4 –CMCH nanoparticles. The characteristic peaks at $2\theta = 30.1^\circ$, 35.5° , 43.1° , 53.4° , 57.0° , and 62.6° for pure Fe_3O_4 nanoparticles, which were marked respectively by their indices (220), (311), (400), (422), (511), and (440), were also observed for Fe_3O_4 –CMCH nanoparticles without and with conjugated papain. This revealed that the surface modification and conjugation of the Fe_3O_4 nanoparticles did not lead to their phase change.

Plots of magnetization versus magnetic field at 300 K for Fe_3O_4 –CMCH nanoparticles without and with conjugated papain are illustrated in Figure 6. The saturation magnetization was found to be 65.4 emu/g for unconjugated nanoparticles and 59.3 emu/g for conjugated nanoparticles. Moreover, the magnetization curves in two cases exhibit nearly zero remanence, which proves the existence of the superparamagnetic character.²⁴ These magnetically active properties of the papain-conjugated Fe_3O_4 –CMCH nanoparticles render them very susceptible to magnetic fields and therefore make the solid and liquid phases separate easily, as demonstrated by Figure 7.

By investigating the hydrolysis of casein as the substrate in the presence of native papain or papain conjugated with Fe_3O_4 –CMCH nanoparticles, the enzyme activity was evaluated at 55 °C and pH 8.0 for native and conjugated papain. For this purpose, the substrate concentration ($[S]$) was plotted against the ratio of $[S]$ to the hydrolysis reaction rate (V) according to the following Hanes–Woolf equation:²⁵

$$[S]/V = (1/V_{\max})[S] + K_m/V_{\max}$$

It was found that such plots could give a good linear relationship between $[S]$ and $[S]/V$ in two cases, as shown in Figure 8. The intercept of the straight line is the ratio of the Michaelis constant (K_m) to the maximum hydrolysis rate (V_{\max}), and the slope of the straight line is the inverse of V_{\max} . In the case of native papain, the K_m and V_{\max} values were found to be 0.5830 g/mL and $142 \mu\text{g mL}^{-1} \text{min}^{-1}$, respectively, together with the corresponding determination coefficient of 0.995. In the case of conjugated papain, the K_m and V_{\max} values were found to be 0.3401 g/mL and $181 \mu\text{g mL}^{-1} \text{min}^{-1}$, respectively, together with the corresponding determination coefficient of 0.992. In contrast, the K_m value of conjugated papain was 1.7 times lower than that of native papain, while the V_{\max} value of conjugated papain was 1.27 times higher than that of native papain. The lower K_m value implies that conjugated papain has a higher affinity to the substrate when compared with native papain.²⁵

The activity retention of native and conjugated papain at different pH values is listed in Table 1. As seen, the pH value has an obvious effect on the enzyme activity of native and conjugated papain. The maximum activity was found to be 7.0 for the native papain and 8.0 for the conjugated papain. At pH 6.0 under the alkaline conditions investigated, however, activity retention of the conjugated papain was higher than that of the native papain, showing an enhanced tolerance to the variation of medium pH. These results might be due to changes in the structure of papain or in the medium pH value after conjugation of papain with the Fe_3O_4 –CMCH nanoparticles.

Table 2 shows the effect of temperature on the enzyme activity of native and conjugated papain. As observed, the activity retention of native and conjugated papain has an obvious difference with the change of temperature. The optimum temperature corresponding to the highest enzyme activity was observed to be 55 °C for the native papain and 75 °C for the conjugated papain. An increase in the optimum temperature of the conjugated papain may result from its relatively extended configuration due to the conjugation process. To understand better the effect of temperature (T) on enzyme activity, Arrhenius plots for the maximum hydrolysis rate (V_{\max}) of casein in the presence of native and conjugated papain were carried out in the temperature range from 25 to 55 °C (Figure 9). It was found that such plots could give a good linear relationship between $\log V_{\max}$ and $1/T$ in two cases, implying that the temperature effect could be described better by the following Arrhenius-type equation:²⁶

$$V_{\max} = A_0 \exp[E_a/(RT)]$$

where E_a is the activation energy, which reflects the sensitivity of the enzyme activity to temperature, and A_0 is a pre-exponential parameter. From the two straight lines shown in Figure 9, the E_a value was estimated to be 13.74 kJ/mol for native papain and 6.95 kJ/mol for conjugated papain. This

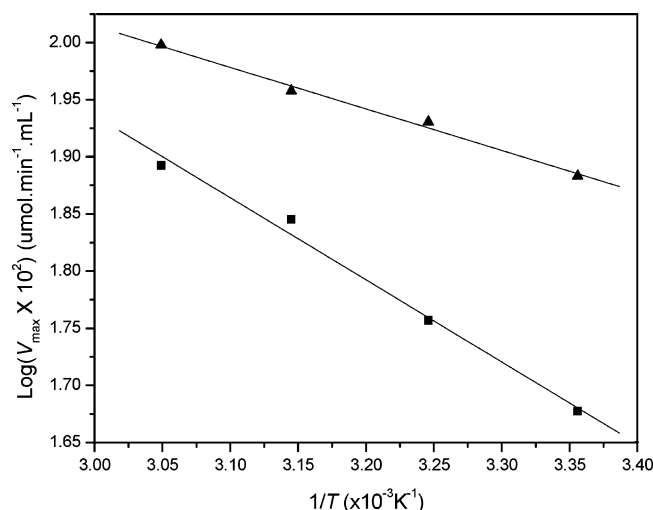


Figure 9. Arrhenius plots for the maximum hydrolysis rate (V_{\max}) of casein in the presence of native and conjugated papain in the temperature range from 25 to 55 °C.

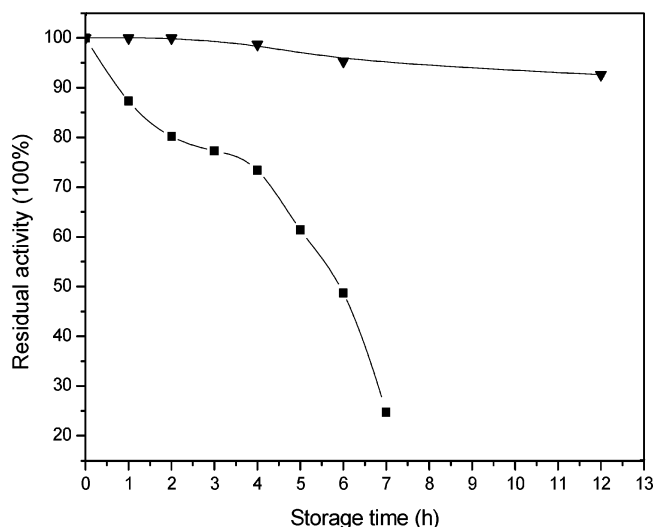


Figure 10. Effects of storage time on the residual activities of native (■) and conjugated (▼) papain (65 °C, pH 8.0).

reveals that papain conjugated with Fe₃O₄–CMCH nanoparticles has a better temperature tolerance when compared with native papain.

Further investigation was focused on the storage stability of native and conjugated papain. As indicated in Figure 10, conjugated papain shows better storage stability in comparison with native papain. For example, activity retention of native papain is only 25% while activity retention of conjugated papain is about 95% after a 7-h standing at 55 °C. In addition, the reusability of conjugated papain was also studied by repeated batch hydrolysis of 2% (w/v) casein in pH 8.0 buffer at 55 °C for 10 min. The residual enzyme activity determined after each cycle decreased slowly. Conjugated papain showed a higher degree of activity recovery, where 81% residual activity was found after eight cycles. In contrast, there is little residual activity for native papain after eight cycles. These results demonstrate that conjugation of papain on Fe₃O₄–CMCH nanoparticles is stable enough to sustain repeated operations or successive use without enzyme inactivation. For papain conjugated with Fe₃O₄–CMCH nanoparticles, good storage stability and high activity recovery may be attributed to fixation of the papain molecules on the magnetic nanoparticles, which prevents autodigestion and/or thermal inactivation of papain.

Conclusions

Superparamagnetic Fe₃O₄ nanoparticles were decorated with carboxymethylated chitosan and then conjugated with papain. It was found that the conjugation process has no significant effects on the size and structure of the Fe₃O₄–CMCH nanoparticles. In comparison with native papain, conjugated papain exhibited enhanced enzyme activity, better tolerance of variations in medium pH and temperature, and improved storage stability as well as good reusability. It is anticipated that such magnetic nanoparticles conjugated with papain may have great potential to serve as a superior support for the immobilization and stabilization of papain.

Acknowledgment. This work was supported by NSFC (20273086; 30470476; 20676155), NSFG (5003252; 039184; 6023103), Department of Science and Technology of Guangdong Province (2004B33101003), and NCET Program (NCET-04-0810) in Universities of China.

References and Notes

- (1) Sangeetha, K.; Emilia Abraham, T. *J. Mol. Catal. B: Enzym.* **2006**, *38*, 171–177.
- (2) Jegan Roy, J.; Sumi, S.; Sangeetha, K.; Emilia Abraham, T. *J. Chem. Technol. Biotechnol.* **2005**, *80*, 184–188.
- (3) Dreuth, J.; Jansonius, J.; Koekoek, R.; Swen, H.; Wolters, B. *Nature* **1968**, *218*, 929–936.
- (4) Solis, S.; Paniagua, J.; Martinez, J. C.; Asomoza, M. *J. Sol-Gel Sci. Technol.* **2006**, *37* (2), 125–127.
- (5) Zhao, B.; Shi, B.; Ma, R. *Eng. Life Sci.* **2005**, *5* (5), 436–441.
- (6) Ganapathy, R.; Manolache, S.; Sarmadi, M.; Denes, F. *J. Biomater. Sci., Polym. Ed.* **2001**, *12* (9), 1027–1049.
- (7) Li, Y. F.; Li, J. R.; Fu, L. D.; Li, Y. Z. *Chin. J. Polym. Sci.* **2001**, *18* (1), 25–31.
- (8) Bhardwaj, A.; Lee, J.; Glauner, K.; Ganapathi, S.; Bhattacharyya, D.; Butterfield, D. A. *J. Membr. Sci.* **1996**, *119* (2), 241–252.
- (9) Eckstein, H.; Renner, H. J.; Brun, H. *Biomed. Biochim. Acta* **1991**, *50* (10–11), S114–S117.
- (10) Hayashi, T.; Hirayama, C.; Iwatsuki, M. *J. Appl. Polym. Sci.* **1992**, *44* (1), 143–50.
- (11) Hayashi, T.; Ikada, Y. *Biotechnol. Bioeng.* **1990**, *35* (5), 518–24.
- (12) Chiou, R. Y. Y.; Beuchat, L. R. *J. Food Biochem.* **1987**, *11* (2), 163–76.
- (13) Pfromm, P.; Wuerges, K. *PCT Int. Appl.* **2006**, p 32.
- (14) Gross, R. A.; Chen, B.; Miller, M. E.; Bohling, J. C. Abstracts of Papers, 230th ACS National Meeting, Washington, DC, Aug 28–Sept 1, 2005.
- (15) Hong, S.; Leroueil, P. R.; Janus, E. K.; Peters, J. L.; Kober, M. M.; Islam, M. T.; Orr, B. G.; Baker, J. R. Jr.; Banaszak, H.; Mark, M. *Bioconjugate Chem.* **2006**, *17* (3), 728–734.
- (16) Halling, P. J.; Dunnill, P. *Enzyme Microb. Technol.* **1980**, *2*, 2–10.
- (17) Huang, S. H.; Liao, M. H.; Chen, D. H. *Biotechnol. Prog.* **2003**, *19*, 1095–1100.
- (18) Dyal, A.; Loos, K.; Noto, M.; Chang, S. W.; Spagnoli, C.; Shafi, K. V. P. M.; Ulman, A.; Cowman, M.; Gross, R. A. *J. Am. Chem. Soc.* **2003**, *125*, 1684–1685.
- (19) Chen, X. G.; Park, H. *Carbohydr. Polym.* **2003**, *53*, 355–357.
- (20) Chang, Y. C.; Chang, S. W.; Chen, D. H. *React. Funct. Polym.* **2003**, *66*, 335–341.
- (21) Bradford, M. M. *Anal. Biochem.* **1976**, *72*, 248–54.
- (22) Tsushida, O.; Yamagato, Y.; Ishizuka, T.; Arai, T.; Yamada, J.; Takeuchi, M.; Ichishima, E. *Curr. Microbiol. J.* **1986**, *14*, 7–12.
- (23) Forato, L. A.; Bernardes-Filho, R.; Colnago, L. A. *Anal. Biochem.* **1998**, *259*, 136–141.
- (24) Son, S. J.; Reichel, J.; He, B.; Schuchman, M.; Lee, S. B. *J. Am. Chem. Soc.* **2005**, *127*, 7316–7317.
- (25) Price, N. C.; Stevens, L. *Fundamentals of Enzymology: The Cell and Molecular Biology of Catalytic Proteins*, 3rd ed.; Oxford University Press: New York, 1999; pp 121–126.
- (26) Zhang, L. M. *Colloid. Polym. Sci.* **1999**, *277*, 886–890.